Specific-Heat Anomaly during Vitrification of Hydrided Fe_2Er Single Crystals

H. J. Fecht, Z. Fu, and W. L. Johnson
W. M. Keck Laboratory of Engineering Materials, California Institute of Technology, Pasadena, California 91125
(Received 15 December 1989)

A solid-state amorphization reaction is observed on hydrided, initially single-crystalline, Fe_2Er powder samples (Fe_2ErH_x, $3.0 < x < 3.4$). Specific-heat measurements at constant concentration ($x = 3.4$) show pronounced premelting effects exhibiting a λ-type transition at $T_c = 475.6$ K and a logarithmic temperature dependence. This typical feature of an instability underlying the "melting" transition has been predicted if the vitrification occurs in the vicinity of the triple point between supersaturated crystal, undercooled liquid, and glass.

PACS numbers: 64.70.Pf, 64.10.+h, 65.40.Hq

As an alternative to liquid undercooling processes, glasses can be synthesized in the solid state by the destabilization and vitrification of crystalline phases through a variety of methods (for reviews, see Ref. 1). Observation of this transition from a nonequilibrium crystalline phase to a glass requires that the formation of crystalline equilibrium compounds be frustrated by the kinetic constraints imposed by the low-reaction temperatures.

The nature of the glass transition (supercooled liquid to glass) is still a matter of controversy, and it has been suggested to be either first-order, second-order, third-order[2] or no phase transition at all, i.e., kinetic freezing.[3] Only recently, an attempt has been made to combine the "melting" transition from crystal to glass with transition (from liquid to glass). A thermodynamic scenario has been developed combining the Kauzmann paradox (an entropy catastrophe which limits the liquid undercooling to the temperature where the liquid and crystal entropies equal[4]) with an entropy catastrophe for melting.[5,6] For binary alloys with negative enthalpy of mixing, the compositional-induced disorder reduces the melting temperature.[7] Imposing polymorphous constraints, i.e., requiring equality of composition in all phases, the melting line (T_0 line with Gibbs-free-energy difference $\Delta G = 0$) should cross the ideal glass transition temperature T_{g0} ($\Delta S = 0$) at a certain composition. Consequently, in analogy to the phase diagrams developed for spin glasses,[8] a triple point with $\Delta G = \Delta S = 0$ may exist between the supersaturated crystal, the undercooled liquid and the ideal glass.[5]

In order to test the validity of these ideas for the melting of a crystal to a glass we studied the hydrogen-induced vitrification of initially single-crystal powder particles of the Laves phase Fe_2Er ($C15$ structure) in the vicinity of the expected triple point. In comparison to other experiments resulting in vitrification of crystalline phases by thermal annealing of multilayers, mechanical alloying or ion-beam irradiation, the hydrogen triggered vitrification has the advantage of allowing two requirements to be fulfilled: (i) elimination of high-energy grain boundaries as heterogeneous nucleation sites that catalyze the formation of the glass phase. These sites would prevent the observation of an instability by triggering glass formation before the instability line is reached, and (ii) suppression of long-range diffusion of the metal atoms. This prevents phase separation and allows one to retain a chemically homogeneous sample, i.e., to maintain the polymorphous constraint (isoconfiguration condition), at the relatively low annealing temperatures compared to the melting point [1633 K for Fe_2Er (Ref. 7)].

The Fe_2Er intermetallic compounds (99.96% purity) were prepared by standard solidification and annealing methods resulting in a single-phase $C15$ structure with a lattice parameter of 7.29 Å and an average grain size of 6 mm. The brittle samples were crushed under an Ar atmosphere to a powder of less than 44 μm diam, thus limiting the number of powder particles containing a grain boundary to a negligibly small amount ($< 10^{-4}$). Crystalline hydrides were subsequently prepared by exposure of the Fe_2Er powder to a hydrogen gas (99.9999%) at constant pressure of 5 atm and temperatures up to 460 K. The metastable crystalline phase supersaturated with hydrogen was subsequently "melted" to a glass following two different routes: (a) by varying the temperature under *isobaric* conditions in a hydrogen furnace at 5-atm hydrogen pressure, and (b) under *isoconcentration* conditions by heating the specimen in a sealed aluminum pan (which is nonpermeable for hydrogen) in a differential scanning calorimeter (DSC). Because of the small excess volume in these pans, the hydrogen content of the sample will change only to a negligibly small amount during heating ($< 1\%$).

Calorimetric measurements were performed using a well-calibrated differential scanning calorimeter (Perkin Elmer DSC4) at scanning rates of 20 K/min. The crystalline samples were cold welded in Al pans using a standard press at a hydrogen overpressure equivalent to the respective furnance pressure. The choice of purge gas (Ar or H_2) turned out to be insignificant for the DSC results. For the precise specific-heat measurements, three subsequent scans were made including an empty Al pan

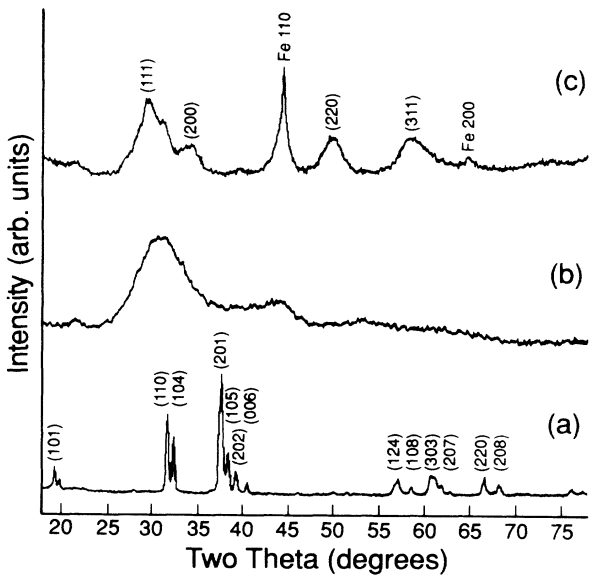

FIG. 1. X-ray-diffraction profiles (Cu $K\alpha$ radiation) with x-ray intensities in arbitrary units for samples prepared under isobaric conditions. (a) The metastable rhombohedral phase $Fe_2ErH_{3.4}$, (b) the amorphous phase $Fe_2ErH_{2.7}$, and (c) the phase-separated stable configuration of ErH_2 and α-Fe.

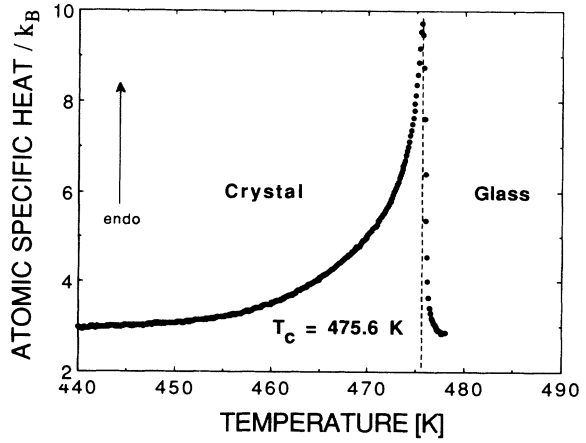

FIG. 2. Differential scanning calorimetry data showing the atomic specific heat c_x at constant concentration as multiples of k_B during the transition from crystalline $Fe_2ErH_{3.4}$ to amorphous $Fe_2ErH_{3.4}$.

of equivalent mass, a sapphire as standard and of the sample itself. The data were collected in temperature intervals of 0.1 K (i.e., $\epsilon = T/T_c - 1 \cong 2\times10^{-4}$) with an accuracy of $\pm 1\%$ or 10^{-4} J/s. The structural analysis was done by x-ray diffraction (Cu $K\alpha$ radiation filtered with a Ni foil) and transmission electron microscopy (Phillips 430 high-resolution microscope at 300 kV).

X-ray-diffraction studies and pressure concentration isotherm analysis reveal the following sequence of phase transformations. Annealing the Fe_2Er samples in the hydrogen atmosphere of 5 atm at temperatures between 370 and 460 K for up to 50 h leads to absorption of hydrogen accompanied with an expansion of the cubic lattice, thus filling all interstitial Fe_2Er_2 and some Fe_3Er tetrahedra sites. For $x > 3.3$ the lattice undergoes a trigonal distortion along the $\langle 111 \rangle$ axis which breaks the fourfold symmetry. This yields a rhombohedral structure (R-3m) as shown in Fig. 1(a) for $x = 3.4$. Compared with the original Laves phase, the final rhombohedral phase exhibits an increase in the total volume of 22% which is rather large in comparison to other hydrides.

Increasing the temperature to 510 K under isobaric conditions results in vitrification of the rhombohedral phase indicated in Fig. 1(b) by the loss of the Bragg-peak intensities and the development of a broadband characteristic for the amorphous structure. This transition is accompanied by a loss of hydrogen to $x = 2.7$. The glassy phase produced by melting of the crystalline phase is stable between 510 and 550 K during the time scales of the experiment. Heating this sample to temperatures above 550 K results in crystallization and phase separation of the initially chemically homogeneous sample into the stable configuration of cubic ErH_2 and α-Fe [see Fig. 1(c)].

The DSC measurements performed on the hydrided crystalline $Fe_2ErH_{3.4}$ powder samples allow one to characterize the "melting process" further. The specific heat c_x at constant concentration collected at a heating rate of 20 K/min is shown in Fig. 2 between 440 and 478 K in units of k_B per atom (k_B is Boltzmann constant). It exhibits an increase of c_x from $2.9k_B$ to $9.7k_B$. A λ-type transition is observed beginning at about 450 K with the critical temperature T_c at 475.6 K (the peak temperature).

TEM micrographs as obtained from powder samples before and after this transition demonstrate a significant change in microstructure. Figure 3(a) shows a high-resolution bright-field image including the corresponding diffraction pattern of the highly strained rhombohedral $Fe_2ErH_{3.4}$ sample prepared at 440 K. After heating this sample in the DSC in a sealed pan to 440 K, no change in the microstructure has been observed. After heating to 480 K, i.e., 2.4 K above T_c, and cooling to room temperature at 20 K/min, a major part of the sample is retained as the amorphous phase as shown in Fig. 3(b). Included in Fig. 3(b) is a diffraction pattern which exhibits the halos typical for the amorphous phase. The remaining part of the sample transformed back to the rhombohedral phase with a much reduced grain size in the nanometer range (5–10 nm) as shown in Fig. 3(c). Thus, the observed λ transition is unambiguously related to the solid-state amorphization process. Other phenomena, the order-disorder transition of the hydrogen atoms on the crystal lattice[9] and the ferrimagnetic to paramagnetic transition[10] are known to occur at lower temperatures (about 330 and 300 K, respectively), and can clear-

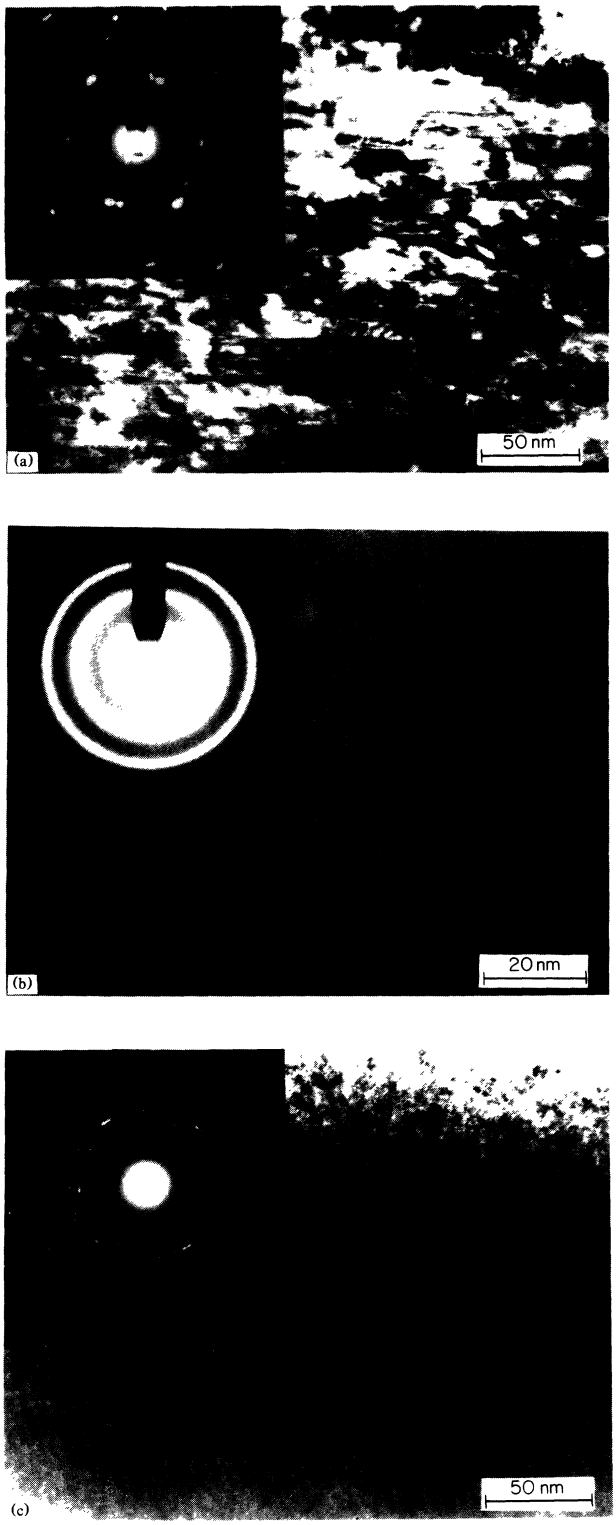

FIG. 3. TEM bright-field images and corresponding diffraction patterns of $Fe_2ErH_{3.4}$ (isoconcentration conditions). (a) Highly strained rhombohedral structure prepared at 440 K, (b) amorphous phase, and (c) nanocrystalline rhombohedral phase after heating sample (a) in the DSC to 480 K and cooling to RT.

ly be ruled out as the cause of the observed anomaly.

The crystal-to-glass transition reported here is not fully reversible as shown by the TEM observations and further DSC data. If a sample is heated to a temperature just slightly below T_c, cooled to room temperature at 20 K/min, and subsequently heated up again, the same pronounced premelting effects are observed, with T_c shifted to a temperature about 5 K below T_c during the first scan. A similar phenomena is observed for a second heating cycle after heating above T_c during the first scan. In this case, T_c is also shifted by about -5 K and the amplitude of the λ transition at T_c is reduced during the second cycle by approximately 30% which is related to the amount of glass phase that is retained during the cooling cycle. During the cooling cycle, the transition is kinetically sluggish and thus smeared over the entire temperature range. Upon heating to temperatures above 480 K, the hydrogen pressure in the sealed pan rises drastically leading finally to the breaking of the seal of the Al pan and the loss of hydrogen from the sample.

The difference in the vitrification temperature (30 K) between the samples prepared under isobaric conditions versus isoconcentration conditions is a consequence of the negative slope of the $T_0(x)$ line. From isobaric cuts through measured p-c isotherms[9] it is known that the hydrogen concentration is decreased with increasing temperature under isobaric conditions. In contrast, for the conditions in the DSC, the hydrogen concentration is kept constant (within 1%). This explains why the crystal-to-glass transition occurs at a lower temperature (higher hydrogen concentration) under isoconcentration conditions if compared to isobaric conditions (lower hydrogen concentration). If the hydrogen concentration is increased above $x=3.4$, the crystal-to-glass transition temperature is decreased even further.[11]

The λ anomaly attributed to the vitrification of the rhombohedral $Fe_2ErH_{3.4}$ phase reflects the topological change of the atomic arrangement indicated by pronounced premelting effects. The nonsymmetric λ-shaped curve in Fig. 2 related to the crystalline phase can be fitted over two decades to a logarithmic specific-heat dependence as $c_x = A\log\epsilon + B$, with $\epsilon = |T/T_c - 1|$ and the critical region for ϵ being less than 0.05. This is shown in Fig. 4 with the background B ($2.9k_B$) subtracted from the measured data and A obtained as $3.405k_B$. Close to the transition (within $\epsilon = 0.001$) rounding of the peak is seen but not followed completely. Such a logarithmic ϵ dependence bears close similarities to the λ transition of ^{4}He (fluid or superfluid) and magnetic transitions close to the critical point.[12] It is interesting to note that the specific-heat data cannot be fitted by a power law with $c_x = A'\epsilon^{\alpha} + B'$ and $\alpha \neq 0$ over reasonably large ranges for ϵ.

These surprising results differ completely from ordinary first-order melting and from calorimetric measurements during vitrification of multilayered thin-film diffusion couples. Melting is in general first order, and

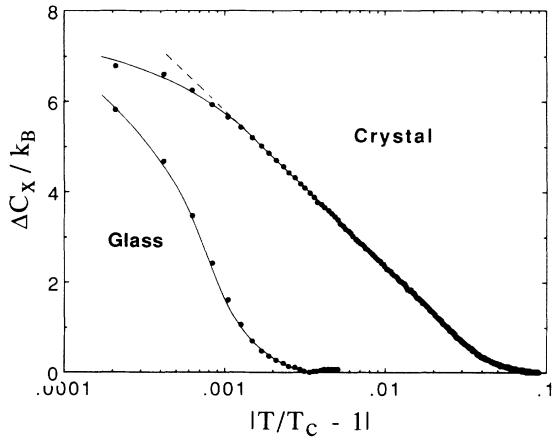

FIG. 4. The heat-capacity difference Δc_x (against the baseline of $2.9k_B$) at constant concentration vs $\log|\epsilon|$ ($\epsilon = T/T_c - 1$) indicating a logarithmic dependence for $\epsilon < 0.05$.

calorimetric measurements indicate a narrow (few degrees) and large signal (in comparison to the specific heat) the area of which is proportional to the heat of fusion. *In situ* measurements of the vitrification of Ni-Zr diffusion couples exhibit an exothermic signal corresponding to the (negative) enthalpy of mixing during diffusion-controlled growth of the amorphous phase.[13]

The observed transition bears close similarities with a crystal that has been severely overheated and melts by an instability.[5,6] For melting, ergodic conditions prevail (i.e., the system can sample *all* configurations in phase space) and the kinetics are very fast, which makes it difficult to observe superheating.[14] In contrast, glasses represent a nonergodic system where equilibrium thermodynamics fails.[3] However, the transition from a highly metastable crystal to a glass can be monitored and appears to be triggered by an underlying instability (possibly an entropy catastrophe). With the strong tendency for phase separation of the solid solution as a driving force for destabilization of the crystalline phase, this technique can be applied further to study the frustration of a first-order transition and the reduction to a truly second-order melting transition.

The financial support from the U.S. Department of Energy (No. DE-FG03-86ER45242), the expert technical assistance of Dr. C. W. Nieh, C. Garland, and H. Lee and stimulating discussions with Dr. R. Bormann, Dr. A. Dommann, Dr. H. Gleiter, Dr. E. Hellstern, Dr. Mo Li, and Dr. K. Samwer are gratefully acknowledged.

[1]W. L. Johnson, Prog. Mater. Sci. **30**, 81 (1986); K. Samwer, Phys. Rep. **161**, 1 (1988).

[2]M. H. Cohen and G. S. Crest, Phys. Rev. B **20**, 1077 (1979); G. Adam and J. H. Gibbs, J. Chem. Phys. **43**, 139 (1965); L. V. Woodcock, J. Chem. Soc. Faraday Trans. 2 **72**, 1667 (1976).

[3]N. O. Birge and S. R. Nagel, Phys. Rev. Lett. **54**, 2674 (1985); P. W. Anderson, in *Ill Condensed Matter,* edited by R. Balian, R. Maynard, and G. Toulous (North-Holland, Amsterdam, 1979), p. 159.

[4]W. Kauzmann, Chem. Rev. **43**, 219 (1948).

[5]H. J. Fecht and W. L. Johnson, Nature (London) **334**, 51 (1988); H. J. Fecht, P. Desré, and W. L. Johnson, Philos. Mag. B **59**, 577 (1989).

[6]J. L. Tallon, Nature (London) **342**, 658 (1989).

[7]T. Massalski, *Binary Alloy Phase Diagrams* (American Society for Metals, Metals Park, OH, 1986), p. 1015.

[8]P. LeDoussal and A. B. Harris, Phys. Rev. Lett. **61**, 625 (1988).

[9]H. A. Kiersteadt, J. Less-Common Met. **70**, 199 (1980).

[10]B. D. Dunlap, G. K. Shenoy, J. M. Friedt, P. J. Viccaro, D. Niarchos, H. Kierstead, A. T. Aldred, and D. G. Westlake, J. Appl. Phys. **50**, 7682 (1979).

[11]K. Aoki, A. Yanagitani, X.-G. Li, and T. Masumoto, Mater. Sci. Eng. **97**, 35 (1988).

[12]L. P. Kadanoff, W. Götze, D. Hamblen, R. Hecht, E. A. S. Lewis, V. V. Palciauskas, M. Rayl, and J. Swift, Rev. Mod. Phys. **39**, 395 (1967).

[13]E. J. Cotts, W. J. Meng, and W. L. Johnson, Phys. Rev. Lett. **57**, 2295 (1986).

[14]S. Williamson, G. Morou, and J. C. Li, Phys. Rev. Lett. **52**, 2364 (1984); J. Däges, J. H. Perepezko, and H. Gleiter, Phys. Lett. A **119**, 79 (1986).

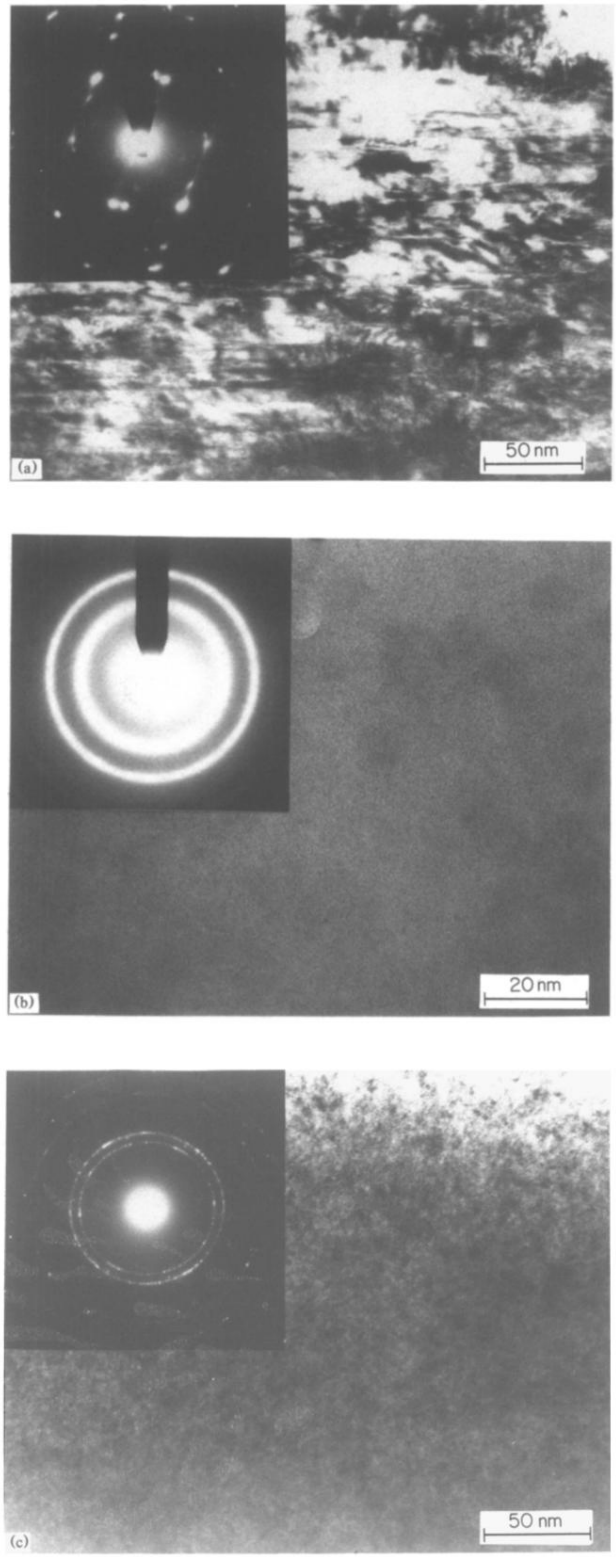

FIG. 3. TEM bright-field images and corresponding diffraction patterns of $Fe_2ErH_{3.4}$ (isoconcentration conditions). (a) Highly strained rhombohedral structure prepared at 440 K, (b) amorphous phase, and (c) nanocrystalline rhombohedral phase after heating sample (a) in the DSC to 480 K and cooling to RT.